PCCP

Probing sulphur clusters in a microfluidic electrochemical cell with synchrotron-based photoionization mass spectrometry

Journal:	*Physical Chemistry Chemical Physics*
Manuscript ID	CP-COM-05-2020-002472.R1
Article Type:	Communication
Date Submitted by the Author:	19-Jun-2020

Complete List of Authors:	Komorek, Rachel; Pacific Northwest National Laboratory , Earth and Atmospheric Sciences Directorate Xu, Bo; Lawrence Berkeley National Laboratory, Chemical Sciences Division Yao, Juan; Pacific Northwest National Laboratory , Atmospheric Sciences and Global Change Division Kostko, Oleg; Lawrence Berkeley National Laboratory, Chemical Sciences Division Ahmed, Musahid; Lawrence Berkeley National Laboratory, Chemical Sciences Division Yu, Xiao-Ying; Pacific Northwest National Laboratory , Atmospheric Sciences and Global Change Division

COMMUNICATION

Probing sulphur clusters in a microfluidic electrochemical cell with synchrotron-based photoionization mass spectrometry

Received 7th May 2020,
Accepted xxth XXXX 2020

DOI: 10.1039/x0xx00000x

Rachel Komorek,[a] Bo Xu,[b] Jennifer Yao,[a] Oleg Kostko,[b] Musahid Ahmed,[b] and Xiao-Ying Yu,*[a]

We present synchrotron-based mass spectrometry to probe products formed in a lithium sulphide electrolyte. *In operando* analysis was obtained at two different potentials in a vacuum compatible microfluidic electrochemical cell. Mass spectral observations show that the charged electrolyte formed sulphur clusters under dynamic conditions, demonstrating electrolyte electron shuttling.

Lithium-sulphur (Li-S) batteries have the potential to provide an inexpensive energy storage solution to support the growing demands of the 21st century such as personal electronics, transportation, and renewable energy. These batteries have several characteristics which make them suitable for implementation into future energy storage solutions, which include high theoretical energy density, abundance, environmental sustainability, and inexpensive production costs.[1] However, drawbacks to their viability as an energy solution include short lifetime, high self-discharge rate, and low charging efficiency.[2] Interest in lithium-sulphur batteries has significantly risen. Thus, a demand to solve problems associated with their use, such as formation of insoluble lithium sulphide (Li_2S_n, $1 \le n \le 8$) in polysulfide electrolytes, has become increasingly important. Real-time and *in operando* analysis is necessary for efficient development of Li-S batteries and Li_2S_n formation under dynamic conditions and can improve understanding and development of Li-S batteries that prevent polysulfide reactions on the Li anode, leading to longer and more efficient battery life.

One of the primary challenges of Li-S batteries lies in the formation of highly reactive Li_2S_n intermediates, which can react with the polymeric binder or other species in side-reactions in the battery. These reactions occur when S_8 clusters are reduced into polysulfide ions as electrons flow from the Li anode to the S cathode, later reacting with the lithium cations (Li^+) that have travelled to the cathode to balance the charge from this ion formation. These Li^+ cations then react with S_n^- clusters to form Li_2S_n, which reacts with the polymeric binder or other species and leads to degradation of the Li anode.[2-4] At present, this polysulfide formation as well as subsequent side reactions are not fully understood, due in part to limitation of tools which allow for *in situ* and *in operando* study of electrochemical reactions.

A recent advance in probing electrochemical reactions with a vacuum compatible microfluidic reactor[5-7] is the System for Analysis at the Liquid Vacuum Interface (SALVI).[8-10] The electrochemical version of SALVI, or the E-cell, utilized for this experiment has a gold (Au) coated thin-film as the working electrode (WE) and two platinum wires as the counter electrode (CE) and reference electrode (RE), respectively, simulating a half cell in a Li-S battery. Using this unique vacuum-compatible interface, real-time monitoring of volatile species formed in the liquid electrolyte at different potentials is possible. The emanating vapor species are photoionized with tunable synchrotron radiation and detected via mass spectrometry allowing for analysis of complex chemistry occurring in the liquid electrolyte.

The SALVI microfluidic reactor and E-cell fabrication details have been described in previous publications.[5, 6, 10] The SALVI block was made by soft lithography using polydimethylsiloxane (PDMS). The E-cell has a reservoir of 2 mm×2 mm with a depth of 300 μm. In order to allow for dynamic control of the electrolyte, three thin wires were used as conductors connecting the Au WE as well as the Pt CE and RE (100 μm diameter), placed in the bottom of the reservoir. Two 2 μm diameter holes 100 μm apart were pre-milled into a silicon nitride (SiN) membrane with the gold thin film WE already sputter coated using a scanning electron microscope with the Focused Ion Beam (SEM-FIB).[11] The holes are necessary to allow the liquid to evaporate from the device under high vacuum (10^{-7} Torr) in the main chamber to become subsequently ionized by

[a] Energy and Environment Directorate, Pacific Northwest National Laboratory, Richland, WA 99354, United States
[b] Chemical Sciences Division, Lawrence Berkeley National Laboratory, Berkeley, CA. 94720, United States.
* Corresponding author: Dr. Xiao-Ying Yu, email: xiaoying.yu@pnnl.gov
Electronic Supplementary Information (ESI) available: [details of any supplementary information available should be included here]. See DOI: 10.1039/x0xx00000x

vacuum ultraviolet (VUV) photons. The SiN window was then irreversibly bonded to the PDMS block by an oxygen plasma treatment. The SALVI E-Cell devices were then sputter coated with a 30 nm gold (Au) thin film over the device so that it could be conductive as one of the electrodes in the ion optics module of the single photon ionization mass spectrometer (SPI-MS),[12] as seen in Fig. 1.

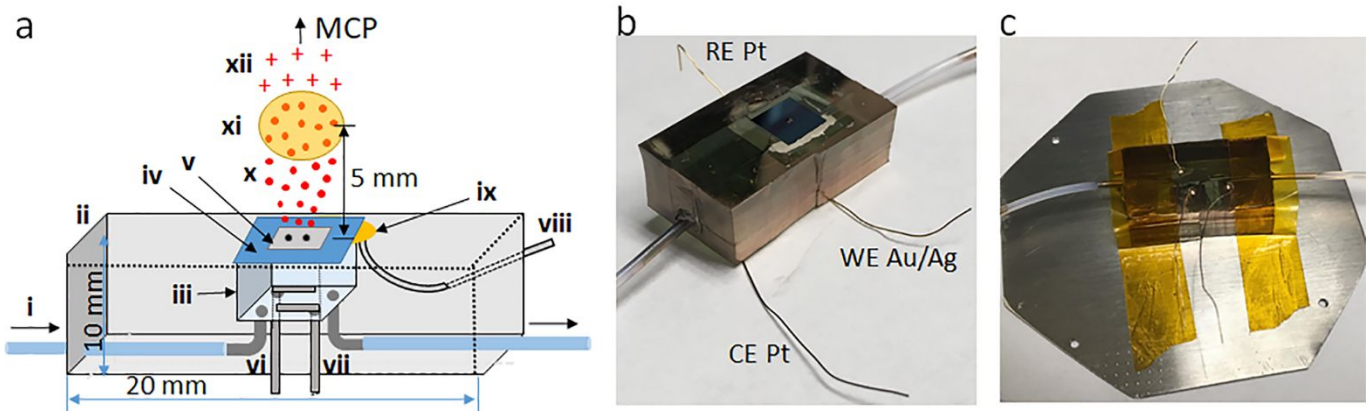

Fig. 1 A schematic showing the SALVI E-cell: a) is a SALVI device, where i) represents the inlet tube and flow direction, ii) is the PDMS block creating the structure of the device, which is coated in Au, iii) is the well which contains the inlet and outlet tubes under the iv) SiN cover with a v) window in the centre which has two 2 µm holes drilled onto it using scanning electron microscopy-focused ion beam (SEM-FIB), as well as the electrodes vi) the Pt counter electrode and vii) the Pt reference electrode. The viii) Au working electrode is bonded to the side of the iv) window with ix) conductive epoxy on an area of the window that is coated with Au, which delivers charge to the top of the channel, underneath the v) window. x) displays the molecules which are evaporated from the 2 µm holes on the window, which crosses the xi) photon beam and becomes xii) positively charged, and are detected with a MCP. b) a photo showing the Au coated SALVI E-cell top-view. c) the SALVI E-cell adapted to the ion optics plate using Kapton® tape.

The Li_2S_8 liquid electrolyte was prepared by following known solution chemistry.[13] The electrolyte was mixed with 1 M of Li_2S_8 into 1 M of dimethoxyethane (Sigma Aldrich, 99.5%, inhibitor free) and 1 M of dioxane (Sigma Aldrich, 99.8%, anhydrous). The electrolyte samples were prepared and packaged in an inert atmosphere to prevent possible oxidation of polysulfide molecules.[14] After injection of the liquid electrolyte into the SALVI E-cell inside a glove box, the device was closed with polyetherketone (PEEK) fittings.

Prior to the experiment, SALVI devices were degassed in a vacuum oven (Thermo Scientific Vacuum Oven, 19.8L, Dial Display, 120V) at 50 °C overnight to reduce the potential interference from the PDMS outgassing due to its permeability.[9] After degassing, the E-cell was then filled with Li_2S_8 solution and fixed to the bottom electrode plate of the ReTOF-MS with ultrahigh vacuum (UHV) Kapton polyimide tape (LewVac, UK) as seen in our earlier work.[12] The SiN membrane was aligned to the centre of the bottom electrode through a 1 mm hole on the adapting plate of ion optics. The distance between the SiN membrane and the VUV light spot was set to ~ 5 mm through height optimization of the mass spectrometer.

The end station at the Chemical Dynamics Beamline (9.0.2) at the Advanced Light Source (ALS), Lawrence Berkeley National Laboratory (LBNL) was coupled to a three-meter VUV monochromator. This apparatus enabled single photon ionization (SPI) representing "soft ionization", which significantly reduced secondary ions or multiphoton ionization.[15] Molecules evaporated from the 2 µm hole of the SiN membrane were ionized by the VUV light and accelerated to the detector. Time-of-flight (TOF) mass spectra were acquired in the photon energy range of 8.5 eV to 12.6 eV at 0.1 eV increments. The photoionization efficiency (PIE) curves were obtained by integrating over the mass peaks at each photon energy and normalizing with respect to photon flux, measured by the silicon photodiode. The first point on the PIE curve which deviated from background signal was taken as the appearance energy (AE) of the molecule, which was compared with literature ionization energy (IE) values to determine if they were in general agreement.

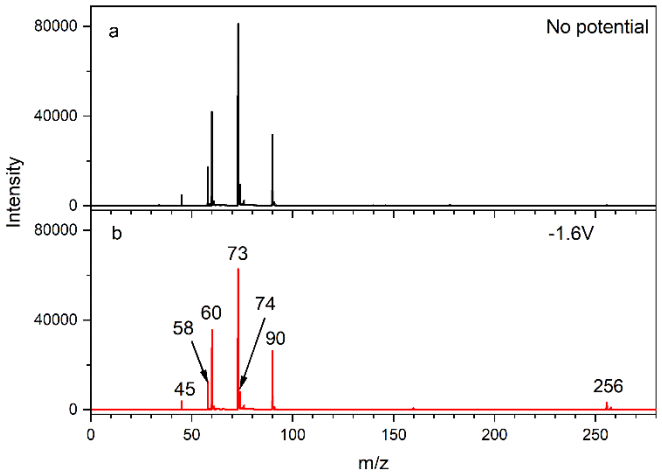

Fig. 2. Observation of the two key components dioxolane (m/z 73, m/z 74) and dimethoxyethane (m/z 90) in the SALVI E-cell (a) without potential applied and (b) with -1.6 V potential applied when the photon energy was set at 10.6 eV. m/z 256 shows the presence of S_8^+ cluster.

Three electrodes were connected to an electrochemical workstation (CH instruments 660d). The connection between the electrochemical workstation and the E-cell was made through a multiport feedthrough in the SPI-MS main chamber including cables linking to the CE, RE, and WE. A potential sweep

or cyclic voltammetry was applied to the E-cell to determine its performance between -2 V and 2V with a scan speed of 0.1 mV/s. Then a constant potential of -1.6 V and 0.2 V was applied subsequently to study the effect of products formed, respectively. It is worth noting that there is a slight potential shift compared to using Li /Li$^+$ due to the use of Pt as the RE. Additional experiments and revised cell designs are needed to simulate a real lithium battery. This approach is more sensitive for detecting species formed at or near the WE as demonstrated previouly.[5-7]

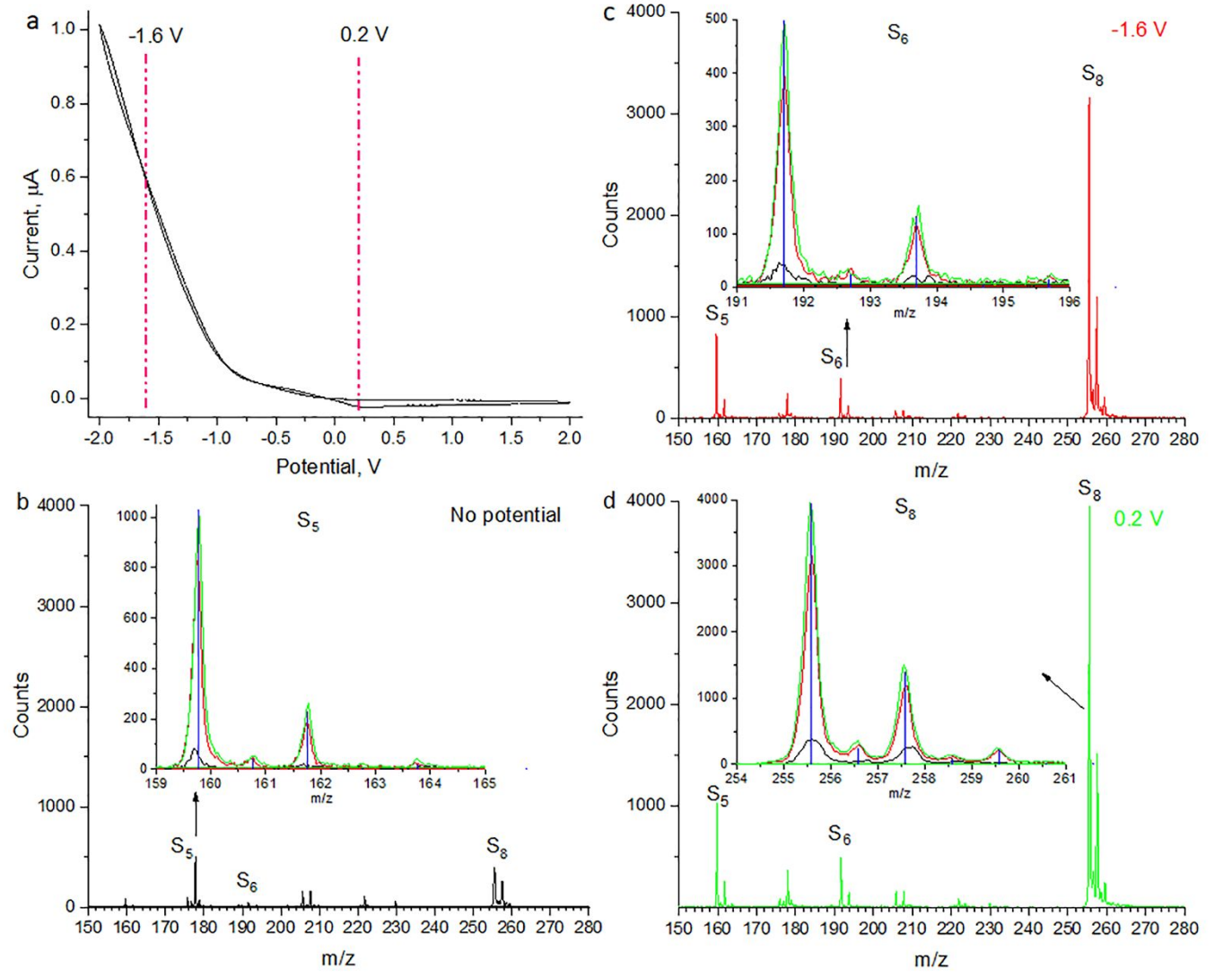

Fig. 3 a) Cyclic voltammogram of the Li_2S_8 electrolyte in the SALVI E-cell and the SPI-MS spectra collected at (b) no potential, (c) -1.6 V, and (d) 0.2 V applied with the photon energy set at 10.6 eV. The inserts in (b-d) depicts the spectral comparisons showing S_5^+, S_6^+, and S_8^+ clusters with sulphur isotopic signatures in the respective mass ranges. The blue lines indicate theoretical locations of sulphur isotopic peaks[16] in each cluster.

Peaks at m/z 45, 58, 60, 73, and 90 are present in the mass spectra with and without voltages applied as shown in Fig. 2 for masses below m/z 120. The peak at m/z 90 originates from the photoionization of the dimethoxyethane ($C_4H_{10}O_2$, MW 90.12), solvent molecule, and m/z 45, 58, and 60, are from dissociative photoionization of the dimethoxyethane ion.[17] The peak at m/z 74 is from the photoionization of dioxolane ($C_3H_6O_2$, MW 74.08), and m/z 73 ($C_3H_5O_2^+$) is from dissociative photoionization as observed in previous electron impact studies.[18] The application of a potential to the SALVI E-cell does not affect the intensity of solvent peaks. This is not surprising as the volatility of the solvent should not be affected by the electron transfer and shuttling of the Li_2S_8 electrolyte.

Figure 3a depicts the cyclic voltammogram of the Li_2S_8 electrolyte under a sweeping potential between – 2 V and 2 V in two cycles. Multiple sweeping cycles showed closed CV results, indicating good performance of the E-cell. The electrochemical performance was compared in the ambient and in vacuo conditions and they showed agreement. We selected two potentials, i.e., -1.6 V and 2 V to hold and probe more the intermediate products formed.

Figures 3b-3d shows the mass spectra between m/z 150-280 recorded at 10.6 eV photon energy, without potential applied and with-1.6 V and 0.2 V potentials applied, respectively. The insets in Figures 3b-d show zoomed in mass ranges to highlight the isotope patterns of sulphur clusters formed at different

potential conditions. As seen in Figure 3d, the sulphur isotope pattern corroborate the identification of S_8^+ clusters while S_5^+ and S_6^+ are identified in the patterns shown in Figures 3b and 3c respectively. Further, the theoretical isotopic sulphur peak locations[16] depicted in blue are compared with the observed peaks. The agreement between the isotopic calculation and observations confirms the dynamic production of sulphur clusters in natural abundance. We compare the appearance of the three sulphur peaks to previous measurements which were performed using vaporization of sulphur and the resulting clusters were ionized with VUV single photon ionization. In contrast to our work, where we only detect S_n (n=5, 6 and 8), the authors in the previous work also detected substantial amounts of n=7 and small amounts of 2, 3 and 4.[19] An early result using VUV photoionization also detected different sizes of sulphur clusters (n=2,3,5,6,7,8) than what was found in our in operando SPI-MS measurements.[20] The lack of observation of reduction products such as S_3 and S_2 is attributed to the low-dielectric electrolyte used in this work.[21] The solvation ability of the solvent is determinant in the observed S-reduction behaviour. In this case, S_3 is not formed in imidazolium ionic liquids as opposed to the reduction steps in high-dielectric electrolytes.[22]

To analyse the difference in mass spectra, we will now turn to our measured photoionization efficiency curves which report on the appearance energies of particular m/z peak. Figure 4 shows the PIE curves for S_5^+, S_6^+, and S_8^+ measured at -1.6 V potential. The S_8^+ PIE curve rises sharply around 9.0 eV, the S_6^+ curve rises slowly around 9.5 eV and then sharply increases at 10.0 eV, while the S_5^+ curve rises sharply at 10.0 eV. The observed AE for S_8^+ agrees very well with an early photoionization measurement of 9.04 eV,[23] and a recent calculated value of 8.99 eV [24] for the adiabatic ionization energy. This would suggest that neutral S_8 clusters are emanating from the electrochemical cell upon voltage application, which are then subsequently being photoionized by the synchrotron. The S_8 clusters are expected to form as a result of Li^+ and S_n^- reactions in the Li-S liquid electrolyte system. The observation therefore is confirming that the *in operando* analysis is possible to capture intermediate species produced in the redox shuttling of polysulfide anions between the electrodes.

The calculations also suggest that the vertical IE (9.48 eV) is close to the adiabatic IE (8.99 eV),[24] which would provide reasonable Frank Condon factors (minimal geometry change upon ionization) and lead to the relatively sharp PIE curve as observed in our experiment. The experimental (8.60 and 9.00 eV)[23, 24] and calculated adiabatic IE's (8.55 and 8.82 eV) for S_5^+ and S_6^+ do not agree with our measured appearance energies of 10.0 eV and 9.5 eV, respectively. This immediately leads us to conclude that these species do not arise from the electrochemical cell, and that they are presumably formed by dissociative photoionization of S_8^+. From theory, the appearance energy of S_6^+ would be 10.08 eV, which would be the sum of the adiabatic ionization energy of S_8^+ (8.99 eV) and fragmentation energy of the following process, $S_8 + h\nu \rightarrow S_6^+ + S_2 + e$ which is calculated to be 1.09 eV.[24] This is in a reasonable agreement with the sharp rise of the PIE curve starting at 10.0 eV observed in our work and in a previous experimental study.[20] The PIE curve for S_6^+ demonstrates a gradual rise starting around 9.5 eV, which can be due to photoionization of neutral S_6 clusters released from the E-Cell. We would expect S_5^+ to arise also from dissociative photoionization, based on the mismatch of the appearance energies seen here and compared to the literature. Indeed, the appearance energy of S_5^+ released from fragmentation of S_8 according to the process $S_8 + h\nu \rightarrow S_5^+ + S_3 + e$ is 10.2 eV, correlating with the AE of 10.0 eV observed here.[23] Based on these observations, we can conclude that the dominant sulphur species ejected from SALVI E-Cell is S_8 and small amounts of S_6. This fact explains drastic difference between mass spectra collected in the current study and mass spectra observed during vaporization of sulphur.

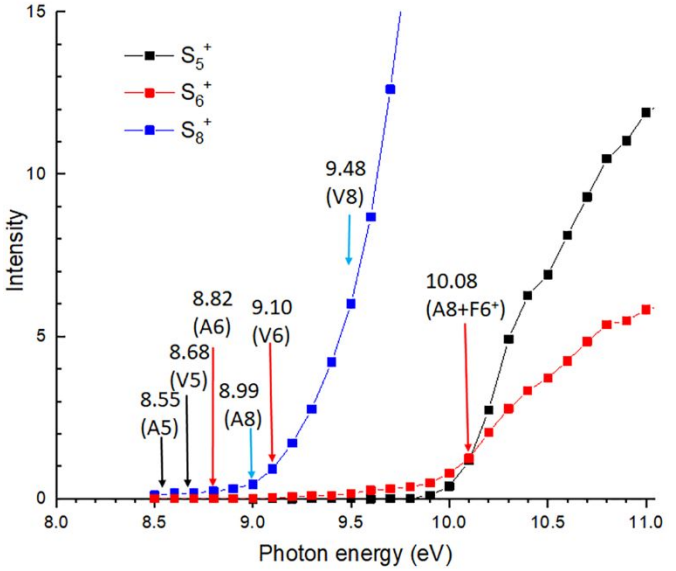

Fig. 4. Photoionization efficiency curves for S_5^+, S_6^+ and S_8^+ measured with CV potential maintained at -1.6 eV. Superimposed are calculated adiabatic (A), vertical (V) ionization energies for S_5, S_6 and S_8 and the sum of fragmentation (F_6^+) from the S_8 Ionization energy adapted from Jin et al.[24]

The first *in operando* electrochemical analysis of Li_2S_8 electrolyte transition under dynamic conditions using VUV SPI-MS has been demonstrated. Using a unique vacuum compatible electrochemical microfluidic interface, real-time monitoring of volatile species formed in the liquid electrolyte at different potentials is possible. The observations from this experiment show that electron shuttling through Li_2S_n can lead to S_n^+ clusters under dynamic conditions. The experiment permits successful determination of the AE values of S clusters and solvent species. Our result showcases the importance of applying gas phase analytical techniques to probe the condensed phase. Future experiments, where the velocity of the emanating vapour beam will be determined, will allow unprecedented access to probe gas-condensed phase interactions and dynamics.

Acknowledgements

The authors were indebted to Dr. Vijayakumar Murugesan for providing electrolytes. RK, JY, and X-Y Y were grateful for the support from the Pacific Northwest National Laboratory (PNNL) Materials Synthesis and Simulation across Scales Initiative (MS^3). This research used resources of the Advanced Light Source, a Department of Energy (DOE) Office of Science User Facility under contract no. DE-AC02-05CH11231. BX, OK, and MA are supported by the Director, Office of Science, Office of Basic Energy Sciences, of the U.S. DOE under Contract No. DE-AC02-05CH11231, through the Gas Phase Chemical Physics Program and Condensed Phase, Interfaces, and Molecular Sciences Program. PNNL is operated for the U.S. DOE by Battelle Memorial Institute under Contract No. DE-AC05-76RL01830.

Conflicts of interest

There are no conflicts to declare.

Key words

sulphur cluster; lithium – sulphur battery electrolyte; in operando analysis; SALVI E-cell; VUV SPI-MS

References

1 S. S. Zhang, *J. Power Sources*, 2013, **231**, 153-162.
2 A. Manthiram, Y. Fu, S. H. Chung, C. Zu and Y. S. Su, *Chem. Rev.*, 2014, **114**, 11751-11787.
3 A. Manthiram, Y. Fu, S. H. Chung, C. Zu and Y. S. Su, *Chem. Rev.*, 2014, **114**, 11751-11787.
4 M. Ling, L. Zhang, T. Y. Zheng, J. Feng, J. H. Guo, L. Q. Mai and G. Liu, *Nano. Energy*, 2017, **38**, 82-90.
5 B. Liu, X. Y. Yu, Z. Zhu, X. Hua, L. Yang and Z. Wang, *Lab Chip*, 2014, **14**, 855-859.
6 J. C. Yu, Y. F. Zhou, X. Hua, S. Q. Liu, Z. H. Zhu and X. Y. Yu, *Chem. Commun.*, 2016, **52**, 10952-10955.
7 X. Y. Yu, B. Liu, L. Yang, Z. Zhu and M. J. Marshall, *USA Pat.,* 20140038224 A1, 2014.
8 L. Yang, X. Y. Yu, Z. H. Zhu, M. J. Iedema and J. P. Cowin, *Lab Chip*, 2011, **11**, 2481-2484.
9 L. Yang, X. Y. Yu, Z. H. Zhu, T. Thevuthasan and J. P. Cowin, *J. Vac. Sci. Technol. A*, 2011, **29**.
10 X. Y. Yu, B. W. Liu and L. Yang, *Microfluid. Nanofluid.*, 2013, **15**, 725-744.
11 X.-Y. Yu, B. Arey, S. Chatterjee and J. Chun, *Surf. Interf. Anal.*, 2019, **51**, 1325-1331.
12 R. Komorek, B. Xu, J. Yao, U. Ablikim, T. P. Troy, O. Kostko, M. Ahmed and X. Y. Yu, *Rev. Sci. Instr.*, 2018, **89**, 115105.
13 R. D. Rauh, F. S. Shuker, J. M. Marston and S. B. Brummer, *J. Inorg. Nucl. Chem.*, 1977, **39**, 1761-1766.
14 M. Vijayakumar, N. Govind, E. Walter, et al., *Phys. Chem. Chem. Phys.*, 2014, **16**, 10923-10932.
15 L. Hanley and R. Zimmermann, *Anal. Chem.*, 2009, **81**, 4174-4182.
16 SCIENTIFIC INSTRUMENT SERVICES, Isotope Distribution Calculator and Mass Spec Plotter, https://www.sisweb.com/mstools/isotope.htm).
17 R. Thissen, C. Alcaraz, O. Dutuit, P. Mourgues, J. Chamot-Rooke and H. E. Audier, *J. Phy. Chem. A*, 1999, **103**, 5049-5054.
18 G. Condecaprace and J. E. Collin, *Org. Mass Spectrom.*, 1972, **6**, 415.
19 J. Varga, S. Wohlfahrt, M. Fischer, M. R. Saraji-Bozorgzad, G. Matuschek, T. Denner, A. Reller and R. Zimmermann, *J Therm. Anal. Calorim.*, 2017, **127**, 955-960.
20 J. Berkowitz and W. A. Chupka, *J. Chem. Phys.*, 1964, **40**, 287-295.
21 Y.-C. Lu, Q. He and H. A. Gasteiger, *J. Phys. Chem. C*, 2014, **118**, 5733-5741.
22 M. Wild, L. O'Neill, T. Zhang, R. Purkayastha, G. Minton, M. Marinescu and G. J. Offer, *Energy Environ. Sci.*, 2015, **8**, 3477-3494.
23 J. Berkowitz and C. Lifshitz, *J. Chem. Phys.*, 1968, **48**, 4346-4350.
24 Y. Jin, G. Maroulis, X. Kuang, L. Ding, C. Lu, J. Wang, J. Lv, C. Zhang and M. Ju, *Phys. Chem. Chem. Phys.*, 2015, **17**, 13590-13597.

TOC

In operando synchrotron analysis captures sulphur clusters' formation and determines their ionization energies in a low-dielectric lithium sulfide electrolyte

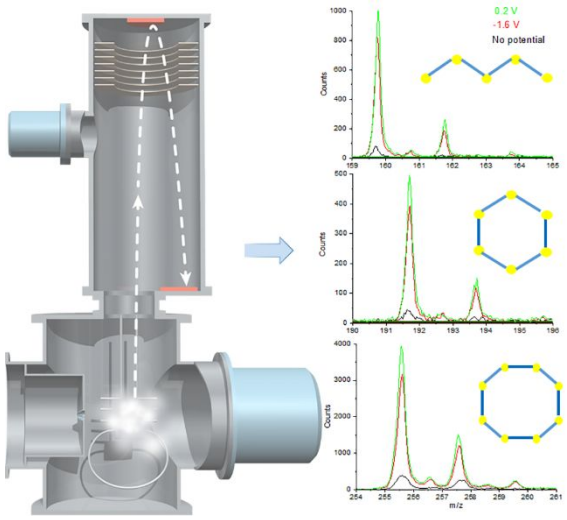

5